Title:
An Approach for Volume Decomposition in Robot-Based Additive Manufacturing

Authors:
Jacopo Lettori, jacopo.lettori@unimore.it, InterMech-DIEF, UNIMORE and UTFPR
Roberto Raffaeli, roberto.raffaeli@unimore.it, InterMech-DISMI, UNIMORE
Milton Borsato, borsato@utfpr.edu.br, UTFPR
Marcello Pellicciari, marcello.pellicciari@unimore.it, InterMech-DISMI, UNIMORE
Margherita Peruzzini, margherita.peruzzini@unimore.it, InterMech-DIEF, UNIMORE

Keywords:
Robot-based Additive Manufacturing, Volume Decomposition, Multi-Slicing Direction

DOI: 10.14733/cadconfP.2022.313-317

Introduction:
Additive Manufacturing (AM) are implemented with robotic manipulators [12] to increase process flexibility in the last decades. Also, researchers have used work tables with certain degrees of freedom [6] for the same aim. Direct Energy Deposition (DED) [9] is one of the solutions for Robot-Based AM (RBAM). The material is deposited from a nozzle onto support [1]. The raw material can be in wire or powder form. Recently, Wire and Arc Additive Manufacturing (WAAM), a form of wire-based DED process, is also gaining interest from both academic as well as industrial point of view. WAAM is an automized welding process where parts are manufactured thanks to a welding gun moved by a manipulator according to 3D paths [14]. The main advantages of WAAM are flexibility, low capital investment, and low material cost [15]. Similarly, extruders for polymeric materials are used in RBAM. Furthermore, RBAM can be integrated with traditional milling solutions to improve the quality of the finished product [11].

RBAM allows the deposition of material along multiple directions [18] thanks to the flexibility of manipulators. Indeed, RBAM overcomes the traditional limit given by the planarity of the manufacturing layer and allows variable slice thickness to be realized.

In general, to maximize realization freedom, part geometry needs to be decomposed into sub-volumes. A suitable slicing strategy is defined for each sub-volume to minimize and possibly remove the need for support [7]. However, software and tools based on this approach are not widespread—commercial systems such as Netfabb, 3DS, and Cura target delta or cartesian AM. In particular, fixed slicing direction is the standard option in the software. There are software specialized in WAAM, such as WAAM3D [21]. However, their use is still limited. Tools for the volume subdivision are lacking, which are a mandatory step for multi-direction deposition. Therefore, ad-hoc algorithms are required to decompose the volume and calculate layers and paths for each of them.

Algorithms for volume decomposition and multi-axis deposition can be found in the literature, such as the Chopper algorithm [4]. This algorithm generates planar separation of an input geometries given the limitations of printer volume. Then, the silhouette curve algorithm [10] divides the initial geometry into a certain number of sub-volumes by evaluating the surface normal at each point. Also, cutting planes algorithms [2], [16] aim at dividing an input geometry to remove the need of overhangs. However, the removal of overhangs can be difficult for some geometries. For example, a beam-guided searching algorithm [16] was used to determine the optimal volume decomposition represented by a sequence of clipping planes. The normals of the planes are the slicing direction of each sub-volume.

The concave loop extraction [7] is another significant approach for volume decomposition.. A series of connected concave edges give a concave loop. These loops are used to divide the part surface in connected regions and the whole solid into sub-volumes [20]. A reference slicing direction is then calculated using the Minimal Enclosing Crown (MEC) algorithm [19]. However, this method strictly depends on a fixed curvature threshold used to find concave loops. Therefore, some sub-volumes may be missed, especially in the presence of non-trivial geometries. On the other hand, the curve skeleton-based algorithm [13] decomposes the volume and finds slicing direction candidates. It uses the 1D medial axis of an input geometry to decompose the volume and find the slicing direction.

The mentioned algorithms look for discrete numbers of sub-volumes and compute a slicing direction for each of them. On the other hand, RBAM can continuously change the deposition direction to perform a continuous deposition. Centroidal axis extraction [8], medial axis [17] and non-uniform [19] algorithms are used to find the optimal processing strategy of a given part portion.

Although approaches for RBAM can be found in the literature, many of them show limits as they cannot be applied for all geometries. Therefore, the research aims to devise a generic tool for volume decomposition and multi-deposition strategy. In particular, this paper presents an algorithm for planar slicing and layers with constant thickness.

Main idea:

The proposed approach is a part of the framework presented in [3]. First, the algorithm performs a preprocessing to simplify the whole part geometry. In particular, holes and small features are removed after being created with standard subtractive processes.

Then, the algorithm performs an in-depth analysis of a sub-volume of arbitrary geometry. At first, the sub-volume is sliced according to an optimal direction chosen as the normal to a planar support base. Layers distance is given as a parameter of the deposition technology. The slicing process defines a sequence of consecutive layers, composed of the intersection of the sectioning planes with the sub-volume boundary.

In particular, three scenarios can occur when two consecutive layers are analyzed (Fig. 1). Note that closed curves form each layer. Inner holes can be present but here neglected for simplicity. A previous layer l_i (black dashed curve) is projected onto the analyzed layer l_{i+1} plane (red solid curve) to analyze the transition from one layer to the next one. As well known, AM technologies require the deposited material to be supported by the previous added material. However, a certain prominence is allowable around the slice contour. Experimental tests have shown that a maximum overhang angle can be assumed according to the selected technology and process parameters [10]. The maximum overhang angle is the value at which external supports are required if the slope of the part exceeds this value. This means that supporting area provided by a previous layer can be determined by an offset of the layer curves toward the outer side (black solid curve) by an amount depending on the layer thickness and the maximum overhang angle. For instance, typical values for the WAAM process can be assumed in a layer height of 3 mm and a maximum overhang angle of 45°.

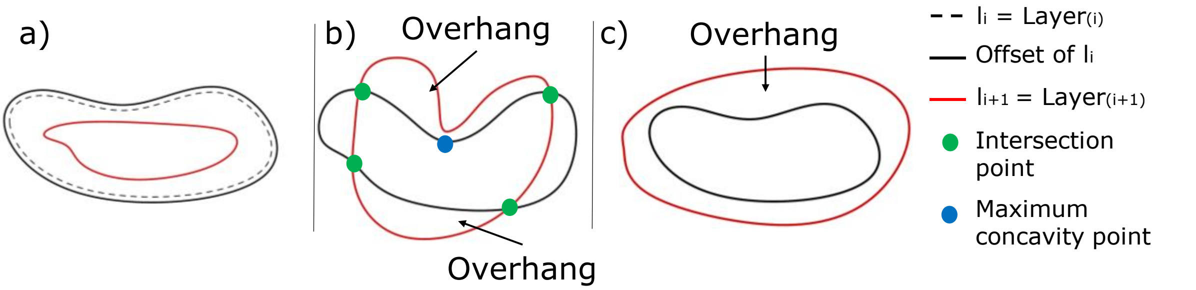

Fig. 1: Scenarios when two consecutive layers are analyzed: a) l_{i+1} is entirely supported by l_i; b) l_{i+1} is not entirely supported, and it intersects the offset of l_i; c) l_{i+1} is not entirely supported, and it does not intersect the offset of l_i.

When one or more overhangs situations are identified, it is necessary to further split the volume in portions that can be manufactured separately without the external supports. The proposed approach provides the separation by separation surfaces whose normals are orthogonal to the current slicing direction.

Assume that the sliced volume in Fig. 2a is the starting geometry. The solid is analyzed layer by layer from the bottom to the top. Initially, each layer is fully supported by the previous one, as in the case in Fig. 1a. When the slope of the lateral surface increases over a threshold angle, the algorithm encounters the scenario depicted in Fig. 1b. Two points are found from the intersection between the offset of l_i and l_{i+1}. Thus, l_{i+1} consists of two parts: a supported area (green solid curve) and an overhang one (red solid curve) as shown in the step 3 of Fig. 2b. The algorithm separates these two parts. Then, it generates the offset of the supported area, as shown in the step 4 of Fig. 2b. This offset is projected onto the next layer, defining the supported area for the next layer. The algorithm iterates these steps until the last layer.

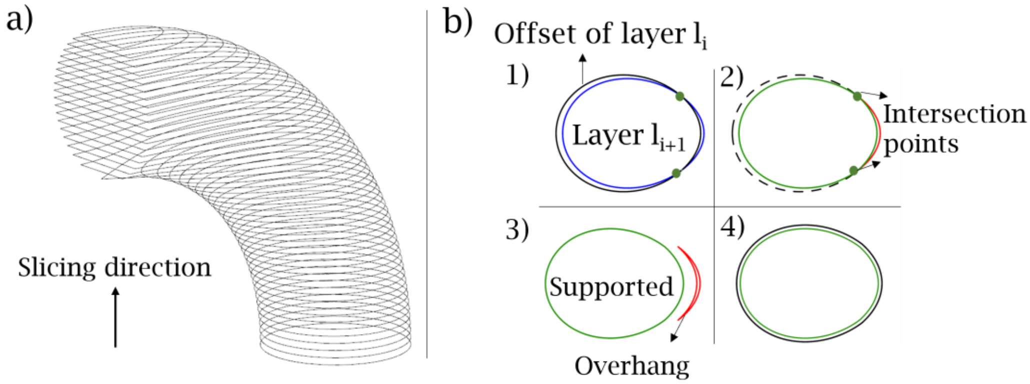

Fig. 2: a) Example of curved sub-volume slicing; b) Layer processing steps.

At the end of the process, from the initial sub-volume supported layers (green curves), unsupported layers (red curves), and the intersections points are identified. From this intermediate result, the algorithm calculates a cutting surface (Fig. 3) made of planar portions to remove from the volume a portion to be subsequently deposited along another direction.

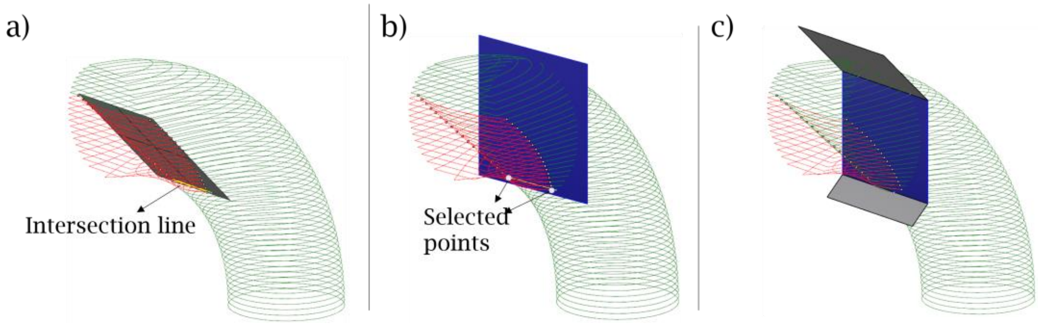

Fig. 3: Computation of the cutting surface: a) Interpolant plane; b) Reference surface; c) Final separation surface composed of the separation surface (blue) and tilted separation surfaces (grey).

First, the algorithm computes an interpolant plane of the intersection points, as shown in Fig. 3a. The plane is intersected with the first layer with an overhang, identifying the line marked in yellow in Fig. 3a. Then, the algorithm builds a plane through this line whose normal is orthogonal to the current slicing direction (Fig. 3b). The plane is translated along its normal to leave all the intersection points on a side. This plane is actually used as subdivision surface. The choice is motivated by the convenience of having a planar base to support the deposition of the detached volume.

The extension of the surface is limited to the layer with overhang portions. Therefore, additional tilted separation surfaces guarantee a complete intersection with the initial sub-volume (Fig. 3c.) The slope of the surfaces is required to avoid collisions between the extruder/torch and the already deposited material. It depends on the geometric characteristics of the extruder/torch, such as the diameter, and the distance between the toolhead and the substrate. Finally, the two obtained sub-volumes and the relative slicing direction are depicted in Fig. 4a.

When the scenario in Fig. 1c occurs, no intersection points are found. In this case, the maximum axis-aligned rectangle inscribed on the layer curve is used to define four separation surfaces [5], as shown in Fig. 4b. The normals of the four surfaces are perpendicular to the original slicing direction (Fig. 4c) and represent the direction of four distinct volume portions to be manufactured. Thus, the rectangle corresponds to the supported and buildable part of the layer. The remaining four volume portions are deposited in an inverse order, i.e., from 4 to 1, to avoid collisions with already deposited material.

If the part presents both scenarios of Fig. 1b and Fig. 1c, the method related to the first encountered scenario is applied. The volume subdivision process is iteratively applied finding new sub-volumes as well as new slicing direction, until all the overhang portions are eliminated.

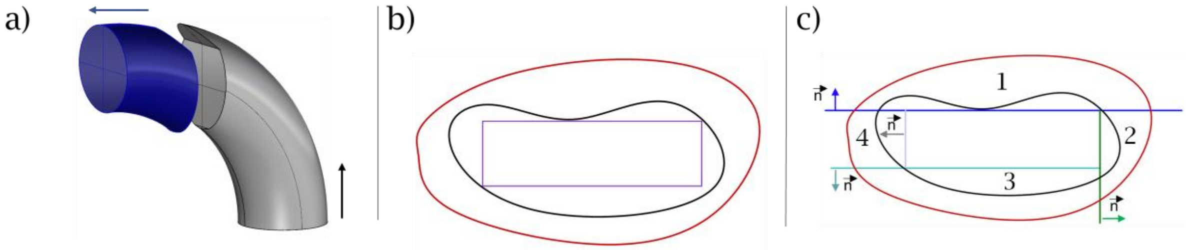

Fig. 4: a) Sub-volumes and slicing directions; b) Maximum axis-aligned rectangle inscribed on the layer curve [5]; c) Separation surfaces generated based on the maximum inscribed rectangle.

Conclusions:

RBAM is a competitive manufacturing solution nowadays. However, software and tools to support the optimization of this process are limited. Hence, this paper presents a method to exploit the flexibility of RBAM and aims to decompose the geometry into sub-volumes that can be deposited without the need of supports.

The process has been successfully applied to some industrial models. It has shown the capability of subdividing the original volume into portions that do not require supports to be deposited.

As future work, layers filling strategies will be analyzed and a process identified to send the required instruction to industrial manipulators equipped with deposition tools. Indeed, the proposed algorithm is still based on planar slicing with constant thickness and does not still fully leverage the capabilities of RBAM. The following steps will include its extension to the deposition of non-constant thickness layers.

References:

[1] Dass, A.; Moridi, A.: State of the Art in Directed Energy Deposition: From Additive Manufacturing to Materials Design, Coatings, 9(7), 2019, 418. https://doi.org/10.3390/COATINGS9070418.

[2] Kanakanala, D.; Swathi, R.; Ruan, J.; Frank, L. X.; Frank, L.: A Multi-Axis Slicing Method for Direct Laser Deposition Process, Proceedings of the ASME Design Engineering Technical Conference, 1(PARTS A AND B), 2010, 425–432. https://doi.org/10.1115/DETC2010-28442.

[3] Lettori, J.; Raffaeli, R.; Peruzzini, M.; Pellicciari, M.: A Framework for Hybrid Manufacturing in

Robotic Cells, Computer-Aided Design & Applications, 19(5), 2022, 1029–1041. https://doi.org/10.14733/cadaps.2022.1029-1041.
[4] Luo, L.; Baran, I.; Rusinkiewicz, S.; Matusik, W.: Chopper: Partitioning Models into 3D-Printable Parts, ACM Transactions on Graphics, 31(6), 2012, 1–9. https://doi.org/10.1145/2366145.2366148.
[5] Marzeh, Z.; Tahmasbi, M.; Mirehi, N.: Algorithm for Finding the Largest Inscribed Rectangle in Polygon, 3(1)(1), 2019, 29–41. https://doi.org/10.22059/JAC.2019.71280.
[6] Rauch, M.; Hascoet, J.-Y.; Querard, V.: A Multiaxis Tool Path Generation Approach for Thin Wall Structures Made with WAAM, Journal of Manufacturing and Materials Processing, 5(4)(4), 2021, 128. https://doi.org/10.3390/jmmp5040128.
[7] Ren, L.; Sparks, T.; Ruan, J.; Liou, F.: Process Planning Strategies for Solid Freeform Fabrication of Metal Parts, Journal of Manufacturing Systems, 27(4), 2008, 158–165. https://doi.org/10.1016/j.jmsy.2009.02.002.
[8] Ruan, J.; Sparks, T. E.; Panackal, A.; Liou, F. W.; Eiamsa-Ard, K.; Slattery, K.; Chou, H. N.; Kinsella, M.: Automated Slicing for a Multiaxis Metal Deposition System, Journal of Manufacturing Science and Engineering, Transactions of the ASME, 129(2), 2007, 303–310. https://doi.org/10.1115/1.2673492.
[9] Saboori, A.; Gallo, D.; Biamino, S.; Fino, P.; Lombardi, M.: An Overview of Additive Manufacturing of Titanium Components by Directed Energy Deposition: Microstructure and Mechanical Properties, Applied Sciences (Switzerland), 7(9), 2017, 883. https://doi.org/10.3390/app7090883.
[10] Singh, P.; Dutta, D.: Multi-Direction Slicing for Layered Manufacturing, Journal of Computing and Information Science in Engineering, 1(2), 2001, 129–142. https://doi.org/10.1115/1.1375816.
[11] Strong, D.; Kay, M.; Conner, B.; Wakefield, T.; Manogharan, G.: Hybrid Manufacturing – Integrating Traditional Manufacturers with Additive Manufacturing (AM) Supply Chain, Additive Manufacturing, 21, 2018, 159–173. https://doi.org/10.1016/j.addma.2018.03.010.
[12] Urhal, P.; Weightman, A.; Diver, C.; Bartolo, P.: Robot Assisted Additive Manufacturing: A Review, Robotics and Computer-Integrated Manufacturing, 59, 2019, 335–345. https://doi.org/10.1016/j.rcim.2019.05.005.
[13] Wei, X.; Qiu, S.; Zhu, L.; Feng, R.; Tian, Y.; Xi, J.; Zheng, Y.: Toward Support-Free 3D Printing: A Skeletal Approach for Partitioning Models, IEEE Transactions on Visualization and Computer Graphics, 24(10), 2018, 2799–2812. https://doi.org/10.1109/TVCG.2017.2767047.
[14] Williams, S. W.; Martina, F.; Addison, A. C.; Ding, J.; Pardal, G.; Colegrove, P.: Wire + Arc Additive Manufacturing, Materials Science and Technology (United Kingdom), 32(7), 2016, 641–647. https://doi.org/10.1179/1743284715Y.0000000073.
[15] Williams, S. W.; Martina, F.: Wire+arc Additive Manufacturing vs. Traditional Machining from Solid: A Cost Comparison; Cranfield; Vol. 32.
[16] Wu, C.; Dai, C.; Fang, G.; Liu, Y. J.; Wang, C. C. L.: General Support-Effective Decomposition for Multi-Directional 3-D Printing, IEEE Transactions on Automation Science and Engineering, 17(2), 2020, 599–610. https://doi.org/10.1109/TASE.2019.2938219.
[17] Xie, F.; Jing, X.; Zhang, C.; Chen, S.; Bi, D.; Li, Z.; He, D.; Tang, K.: Volume Decomposition for Multi-Axis Support-Free and Gouging-Free Printing Based on Ellipsoidal Slicing, Computer-Aided Design, 143, 2022, 103135. https://doi.org/10.1016/j.cad.2021.103135.
[18] Xu, J.; Gu, X.; Ding, D.; Pan, Z.; Chen, K.: A Review of Slicing Methods for Directed Energy Deposition Based Additive Manufacturing, Rapid Prototyping Journal, 24(6), 2018, 1012–1025. https://doi.org/10.1108/RPJ-10-2017-0196.
[19] Zhang, J.; Liou, F.: Adaptive Slicing for a Multi-Axis Laser Aided Manufacturing Process, Journal of Mechanical Design, Transactions of the ASME, 126(2), 2004, 254–261. https://doi.org/10.1115/1.1649966.
[20] Zhao, G.; Ma, G.; Feng, J.; Xiao, W.: Nonplanar Slicing and Path Generation Methods for Robotic Additive Manufacturing, International Journal of Advanced Manufacturing Technology, 96(9–12), 2018, 3149–3159. https://doi.org/10.1007/s00170-018-1772-9.
[21] WAAM3D, https://waam3d.com/.